Withstanding the wind

Joseph D. Smith, Missouri University of Science and Technology, USA, Robert Jackson, Vikram Sreedharan and Ahti Suo-Anttila, Elevated Analytics, LLC, USA, and Doug Allen and Scot Smith, Zeeco, Inc., USA, discuss the safe operation of adjacent multi-point ground flares, focusing on predicted and measured flame radiation in cross flow wind conditions.

Low profile multi-point ground flares (MPGF) represent a special class of flares capable of safely processing significant quantities of flare gas in an environmentally responsible fashion. A detailed computational fluid dynamics (CFD) model of three low profile multi-point ground flares located in close proximity (Figure 1) has been developed using a flare modelling tool called *C3d*. This CFD tool has also been used to simulate many other flare systems, including enclosed flares, elevated steam and air-assisted flares, pressure-assisted flares, and other MPGFs. The MPGF system outlined in this article is part of a chemical production plant located on the US Gulf Coast. The present system included three MPGFs (ethylene: 756 tips/4.1 million lb/hr/22 Ave MW; low density polyethylene (LPDE): 115 tips/ 500 000 lb/hr/28 Ave MW; and linear low density polyethylene (LLDPE): 80 tips/280 000 lb/hr/32 Ave MW).

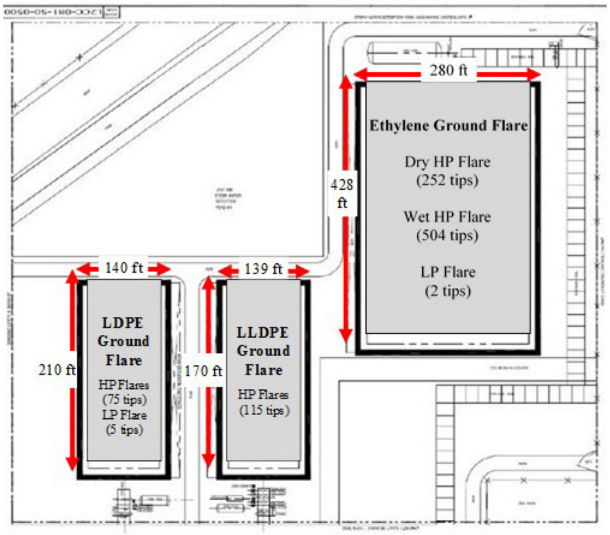

Figure 1. Plan view of MPGF and structures included in the CFD model.

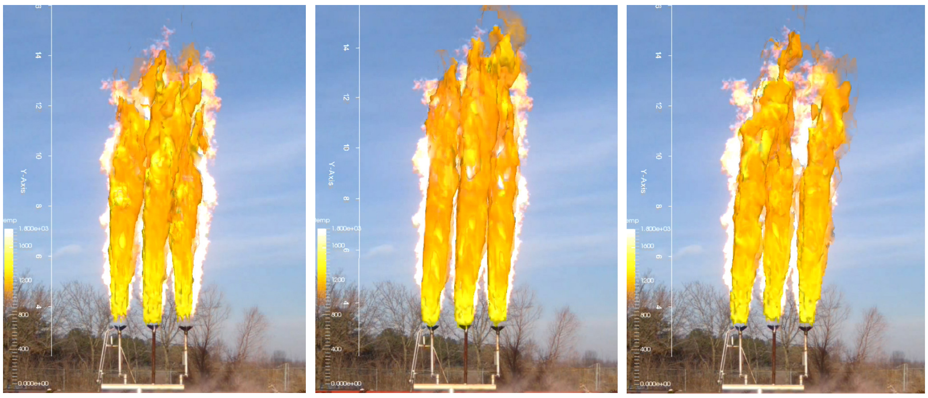

Figure 2. Comparison of predicted and measured flame shape for the three flare test (sequential predicted images overlaid to test flame).

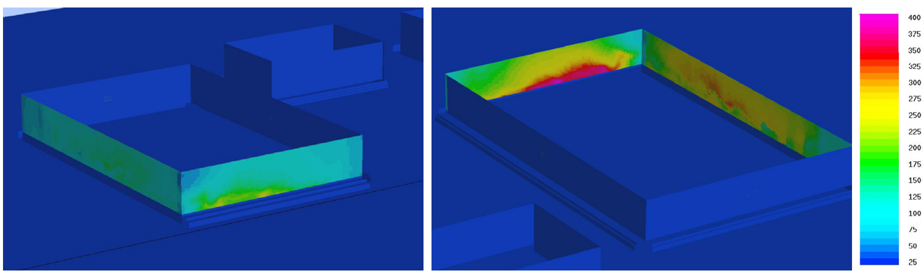

Figure 3. Ethylene flare fence temperatures: a) outer fence surface; b) inner fence surface.

Safety issues related to the MPGF's impact on surrounding structures and personnel were analysed using CFD to examine radiation levels, potential over pressure caused by ignition delay and flare plume dispersion for different wind directions/speeds and firing rates.

Previous validation work has been carried out to assess the accuracy of the flare model, and the combustion scheme used in the flare model.[1, 2] The information presented in this article describes the approach used to assess safety issues for large scale MPGF operation.

The flare model

Analysing an MPGF using CFD requires simulation of turbulent reaction chemistry coupled with radiative transport between buoyancy driven fires (i.e. pool fires, gas flares, etc.) and surrounding objects (i.e. wind fence, process equipment, etc). The CFD tool must 'reasonably' estimate various risk scenarios including wind, percentage flame coverage and thermal fatigue over large domains. The code used in the present work (*C3d*) is based on an earlier tool called ISIS-3D,[3 - 5] which was previously validated for pool fires.[6 - 9] *C3d* has successfully simulated multi-point ground flares, air-assisted flares and utility flares with combustion models tested for methane, ethane, ethylene, propane, propylene and xylene. *C3d* simulations of flame height and flame-to-ground radiation have been validated by direct comparison to measured flare flame size, shape and radiation flux from single and multi-burner tests for no wind and low wind conditions.[10] For the present work, *C3d* has been used to analyse maximum flow at a variety of wind directions for the multi-flare system (Figure 1). The over pressure potential due to delayed ignition in a few of the stages has been analysed. Wind fences can create unexpected flow profiles inside the flare field, which affects combustion and plume dispersion. This can also dramatically affect radiation levels to surrounding structures. CFD analyses have been used to investigate these safety concerns for the system shown.

Technical approach

Practical analysis of the flare field required approximating the detailed fence and burner design to limit the computational cells required and the associated central processing unit (CPU) time to perform the analysis. Structured Cartesian grids were developed for both the overall multi-MPGF flare system and the individual MPGF flares. Grid refinement improved calculation robustness and convergence speed and assured grid independent results. The grid for

Table 1. **Comparison of predicted and measured radiation fluxes at six locations for two wind speeds**

Wind speed	3 - 7 mph	5 mph	10 mph	3 - 7 mph	5 mph	10 mph
Elevation	5 ft	5 ft	5 ft	20 ft	20 ft	20 ft
Measured/ predicted	Measured	Predicted	Predicted	Measured	Predicted	Predicted
Radiometer distance from flare	Measured flux (Btu/hr-ft^2)	Predicted flux (Btu/hr-ft^2)	Predicted flux (Btu/hr-ft^2)	Measured flux (Btu/hr-ft^2)	Predicted flux (Btu/hr-ft^2)	Predicted flux (Btu/hr-ft^2)
75 ft	171	190	168	205	221	183
100 ft	102	117	95	102	120	104
150 ft	34	53	38	34	53	38

Table 2. **Receptor radiation levels and metal temperatures**

Receptor No.	Receptor elevation	Metal type	Total radiation (Btu/hr/ft^2)	Receptor metal surface temperature (°C)
21	45 ft - 6 in.	CS	4	32
22	69 ft	CS	4	32
25	63 ft - 2 in.	CS	88	35
26	54 ft - 3 in.	SS	69	42
27	80 ft - 3 in.	SS	105	48

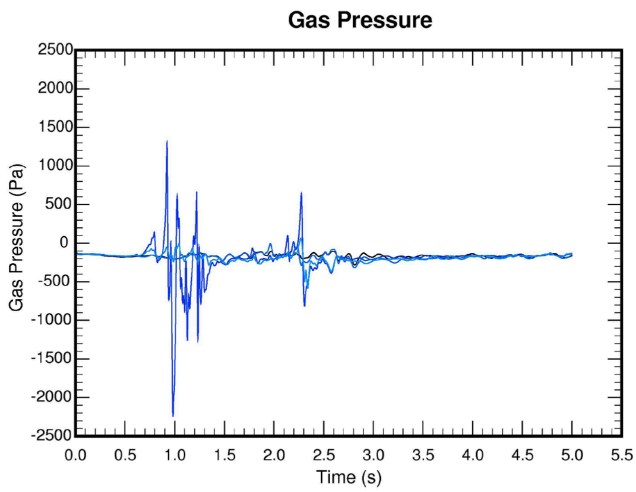

Figure 4. Over pressure predictions at various locations as a function of time on the wind fence for the worst case scenario (perpendicular wind blowing upstream, ignited stage to unignited stage).

the combined MPGF system required 11.5 million cells (with refinement near burners and regions with high flow gradients) while the grid for the single ethylene MPGF required 4.5 million cells.

Combustion model

The combustion model described initially by Said et.al.[13] and used for earlier flare analyses[1, 2] includes fuel (H_2 and C_2H_4), oxygen (O_2), products of combustion (PC) from complete combustion (H_2O and CO_2), radiating carbon (soot), and other non-radiating intermediate species (H_2, CO and C_2H_2). Specific reactions considered included:

- Combustion reaction 1:
  - $H_2 + 8O_2$ --> $9H_2O$ + 141 MJ/kg ($A_k = 10^{15}$, T_a = 10 500K)
- Combustion reaction 2:
  - $CO + 0.57[O_2]^{1/2} + 0.64[H_2O]^{1/2}$ --> $1.57CO_2 + 0.64H_2O$ + 10.1 MJ/kg ($A_k = 10^{13}$, T_a = 15 151K)
- Combustion reaction 3:
  - $[C_2H_4]^{1/2} + 0.769O_2$ --> $0.769H_2O + 0.801C_2H_2$ + 11.5 MJ/kg ($A_k = 10^{15}$, T_a = 10 500K)
- Combustion reaction 4:
  - $[C_2H_2]^{1/2} + 2.46O_2$ --> + $2.62CO_2 + 0.588H_2O$ + 0.3 soot + 29.2 MJ/kg ($A_k = 10^{15}$, T_a = 15 500K)
- Combustion reaction 5:
  - Soot + $1.33O_2$ --> 2.33CO + 13.6 MJ/kg ($A_k = 10^{15}$, T_a = 13 590K)

Where coefficients (based on kilograms of reactant) are selected for complete soot combustion and the intermediate species produce the same species and thermal energy as direct fuel combustion. The flare gas Arrhenius combustion time scale is combined with the turbulence eddy breakup time scale to yield an overall reaction rate time scale:

$$t_{total} = t_{arrhenius} + t_{turb} = 1C^{i} = 1A_k T^b exp - T_a/T + C_{eb}\Delta x^2 \varepsilon_{diff}$$

Where A_k = pre-exponential coefficient, T_A = activation temperature, T = local gas temperature, and b = global exponent, Δx = characteristic cell size, C_{eb} (user specified) is cell size dependent, ε_{diff} = eddy diffusivity from turbulence model, and t_{turb} = turbulence time scale. This simplified combustion model correctly approximates turbulent reacting flow using the eddy dissipation concept and local equivalence ratio effects.

To minimise CPU time, the minimum number of reactions that balance requirements of total energy yield and species consumption and production are used. A multi-step chemical reaction to approximate the global reaction mechanism and ensure the conservation of energy and chemical species is used.

The present work relied on earlier work by Duterque et. al.[15] and Kim,[16] and used the global reaction mechanism described by Smith et. al.,[2] but the pre-exponential coefficients for all reactions were varied to match observed flame shape and soot formation. *C3d* relies on a large eddy simulation (LES) formulation to approximate turbulent mixing, which depends on the proportionality coefficient and cell size. The proportionality coefficient was set as 0.15 and the cell size was set by calibrating the results to the triple ethylene flare radiation and flame size measurements (Figure 2).

To analyse the ignition/over pressure cases, a new ignition model was developed that simulated propagation of a deflagration wave using a user input propagation speed, which is the minimum velocity a deflagration wave could have. Deflagration propagation through the vapour cloud occurs at this speed or greater, except when the vapour cloud is large enough so that hot gas expansion causes adjacent cells to ignite faster than the propagation velocity, which accounts for flame acceleration. Ethylene deflagration velocity (20 - 40 m/sec.) was established from the literature for unobstructed large clouds,[17] as observed for large lenticular shaped balloons (~10 m length) of ethylene gas.

Radiation validation

Radiation validation simulations were performed for propylene fuel using 2 in.[2] ground flare nozzles. The test used a single tip with 5465 lb/hr propylene flowing at 22.5 psig with a 3 - 7 mph crosswind (gusting to 9 - 13 mph). Radiation measurements were taken at 75 ft, 100 ft and 150 ft, and at 5 and 20 ft elevations. Radiometers were placed due east of the flare with wind from the south southeast (SSE), 169˚ from true north. Flare radiation was previously found to be very sensitive to wind velocities[1] with higher radiation fluxes measured under low wind than for high winds. Wind velocity chosen for the validation cases were 5 and 10 mph. Simulations included atmospheric absorption by CO_2 and H_2O using the Hamins and Fuss correlation.[9] Results shown all fall within the predicted band limited by the two wind speeds. This data also reconfirms how sensitive flare radiation is to wind speed.

Modelling basis

For this work, flare gas combustion was described by the chemical reaction mechanism discussed earlier. Process conditions used in the model (wind speed, flare gas inlet temperature/pressure and composition) were set to match expected plant conditions. Model boundary conditions included wind velocity on the upwind side of the domain with pressure boundaries used on all other boundaries except the ground. Thermal and species boundary conditions were set for each case using typical air composition and average ambient temperature at 73˚F (23˚C).

C3d includes sub-models to predict flame emissivity as a function of gas composition, soot volume fraction, flame size/shape and temperature (which depends on mass, momentum, energy and species transport). The radiation transport model predicts radiation flux to surrounding surfaces and provides source and sink terms to the energy equation so flame temperature can be accurately predicted.

Thermal radiation is predicted inside the flame zone, assuming it is diffusive and outside the flame zone using transient view factors. The flame surface used in this calculation is determined by finding a dynamic surface with a mass fraction above/below the user specified value. This information is used to calculate view factor radiation from all flame surfaces to surrounding surfaces, including process instruments and equipment, and can also be used to establish safe work zones. View factor radiation calculation includes shadowing and radiation absorption by participating media (water vapour, carbon dioxide and soot) along the ray path.

Transient calculation and post-processing results

When simulating an operating MPGF, a steady wind profile must be established. This is accomplished by running the transient simulation for sufficient time to allow the inlet wind to propagate across the flare field, plus an additional 10 to 15 seconds before firing flare gas into the flare field. With an established wind profile and flare gas ignited and burning, the simulation is then allowed to burn for about 17 seconds to capture flame fluctuations caused by interactions between adjacent burners and the wind. Convergence criteria used for these simulations were set so the equation of state had to be satisfied to within 0.01% or less throughout the computational domain. Convergence was normally better than the maximum allowable, since time step constraint was limited by Courant conditions, which allowed the flow field to be more accurately solved.

Results

All three flares shown in Figure 1 were analysed individually for multiple wind conditions. Analyses were also performed with all three flares operating simultaneously, under multiple wind conditions. The safe operation of MPGFs was analysed using results from the ethylene flare, operating by itself with a 20 mph (8.9 m/s) cross wind. Flare gas flowrate was set as 4.1 million lb/hr, with flare gas composed of ethylene and 11 - 20% hydrogen. Radiation predictions were provided at 30 unique receptors located around the flare field where staff might work or key plant equipment might be located. Five receptors (21, 22, 25, 26 and 27) represented key locations based on wind direction and resulting flare plume.

The predicted inner fence surface temperatures were highest near the downwind corner (Figure 3b). Since the analysis considered heat conduction through the fence slats and re-radiation from the fence to the surroundings, the outer fence temperatures were predicted to be lower (Figure 3a). Radiation levels at the five critical receptors are summarised in Table 2. Predictions consider radiation flux from the flame and the hot plume and include convective heat gain/loss from the receptors. The total radiation flux to each receptor is predicted to be less than 500 Btu/hr/ft^2 (the safe level recommended by the American Petroleum Institute [API]).

The potential for an over pressure wave being generated by delayed ignition is a significant safety concern. Potential scenarios, considered very unlikely, were considered to reduce insurance risk profile associated with the flare system (using CFD to examine potential risk as a way to reduce the insurance risk profile was recommended at the 2015 AFRC meeting held in Salt Lake City, which resulted in the formation of the API Academic Liaison

Sub-Committee). Previous work showed that very short ignition delays (< 150 ms) at maximum flare gas flow could generate significant over pressure conditions (> 7 psig) that could damage nearby equipment and structures and harm plant personnel working in the vicinity.[2] The scenario presented considered stages 1 - 4 burning, but, due to an assumed inoperable pilot, stage 5 was considered to be venting flare gas to the atmosphere and remained unignited, allowing a cloud of unignited flammable flare gas to form and disperse above the tips, based on the direction the ambient wind was assumed to be blowing. Cases where the wind was blowing parallel to the burner row, as well as when the wind was blowing perpendicular to the burner row, were analysed. Flare gas dispersion based on 0.6 seconds venting prior to Stage 5 ignition was analysed to identify how the flammable cloud ignited and burned using the transient nature of the LES simulation. This analysis was conducted to estimate how large the unignited flammable plume might become, and what happened after ignition occurred for each wind condition. After ignition occurred, the predicted pressure created by the deflagration was predicted to establish the potential risk to surrounding equipment (i.e. fences, buildings, etc.) and to nearby plant personnel.

The scenario with the wind blowing perpendicular to stages resulted in a maximum peak over pressure of approximately 1400 Pa (0.2 psi) for a total of eight different wind conditions with various flare operating scenarios considered. The predicted pressure profiles as a function of time at various locations on the fence are shown in Figure 4.

Conclusion

The transient LES-based CFD tool, *C3d*, was used to assess safety issues related to the performance of multiple large MPGFs located in close proximity to each other. Issues considered included the predicted radiation flux (and associated temperatures) at several nearby receptors, as well as the resulting plumes from each of the flares at maximum venting conditions for 20 mph (8.9 m/sec.) wind coming from multiple directions. Results from the largest of the three MPGFs, for what was considered the most critical wind condition, were used to illustrate how CFD can be used to assess safety risks related to fence temperatures, radiation levels at key equipment locations, plume dispersion and potential over pressure waves produced by delayed ignition of the MPGFs for selected wind conditions. Simulations predicted the average temperature of the inner fence surface was on average 275°C (maximum of 400°C). As expected, the MPGF fence shielded nearby structures from radiation, reducing heat flux by up to a factor of three or more. Several wind conditions were considered to examine how wind affects the flare plume blowing toward surrounding structures, and how this increases the heat flux to various nearby receptors, with predicted levels determined to remain below 110 Btu/hr-ft^2. Several unignited stage over pressure scenarios were analysed, with the highest predicted over pressure level being approximately 1400 Pa (0.2 psi). Results from this study were used to evaluate the proposed MPGF system design and help evaluate key safety concerns, which may be used to reduce the insurance risk profile for the plant, thus impacting the financial performance of the new flare system.

Based on this work, it is recommended that this type of analysis is used to investigate safety issues surrounding existing MPGF systems for normal operating conditions to re-evaluate their risk profiles. Flare vendors such as Zeeco routinely apply CFD to evaluate potential operating scenarios for their design before the flares are built. However, this work illustrates the potential value to companies that own and operate MPGFs, in terms of analysing their systems under worse case scenarios, to investigate potential safety hazards that may reduce their insurance risk portfolio and lower insurance costs.

References

1. SMITH, J. D., SUO-ANTTILA, A., SMITH, S. K. and MODI, J., 'Evaluation of the Air-Demand, Flame Height, and Radiation Load on the Wind Fence of a Low-Profile Flare Using ISIS-3D', AFRC-JFRC 2007 Joint International Combustion Symposium, Marriott Waikoloa Beach Resort, Hawaii, 21 - 24 October 2007.
2. SMITH, J. D., SUO-ANTTILA, A., PHILPOTT, N. and SMITH, S., 'Prediction and Measurement of Multi-Tip Flare Ignition', Advances in Combustion Technology: Improving the Environment and Energy Efficiency, American Flame Research Committees - International Pacific Rim Combustion Symposium, Sheraton Maui, Hawaii, 26 - 29 September 2010.
3. SUO-ANTTILA, A., WAGNER, K. C. and GREINER, M., 'Analysis of Enclosure Fires Using the Isis-3DTM CFD Engineering Analysis Code', Proceedings of ICONE12, 12th International Conference on Nuclear Engineering, Arlington, Virginia, USA, 25 - 29 April 2004.
4. GREINER, M. and SUO-ANTTILA, A., 'Validation of the ISIS Computer Code for Simulating Large Pool Fires Under a Varity of Wind Conditions', ASME J, Pressure Vessel Technology, Vol. 126, 2004, pp. 360 - 368.
5. GREINER, M. and SUO-ANTTILA, A., 'Fast Running Pool Fire Computer Code for Risk Assessment Calculations', presented at the ASME International Mechanical Engineering Congress and Exhibition, 15 - 21 November 2003, Washington, DC.
6. GREINER, M., ARE, N., LOPEZ, C. and SUO-ANTTILA, A., 'Effect of Small Long-Duration Fires on a Spent Nuclear Fuel Transport Package', Institute of Nuclear Materials Management 45th Annual Meeting, Orlando, FL, 18 - 22 July 2004.
7. Society Fire Protection Engineers, 1995, Fire Protection Engineering, 2nd Edition, National Fire Protection Association Publication.
8. GREINER, M. and SUO-ANTTILA, A., 'Radiation Heat Transfer and Reaction Chemistry Models for Risk Assessment Compatible Fire Simulations', Journal of Fire Protection Engineering, Vol. 16, 2006, pp. 79 - 103.
9. FUSS, S. P. and HAMINS, A., 'An estimate of the correction applied to radiant flame measurements due to attenuation by atmospheric CO_2 and H_2O', Fire Safety Journal, Vol. 37, 2002, pp. 181 - 190.
10. SUO-ANTTILA, A. and SMITH, J. D., 'Application of ISIS Computer Code to Gas Flares Under Varying Wind Conditions', 2006 American Flame Research Committee International Symposium, Houston, Texas, 16 - 18 October 2006.
11. SMITH, J. D., JACKSON, R., SUO-ANTTILA, A., HEFLEY, K., WADE, D., ALLEN, D. and SMITH, S., 'Prediction and Measurement of Multi-Tip Flare Ignition', American Flame Research Committees 2013 – Industrial Combustion Symposium, Safe and Responsible Development in the 21st Century, Sheraton Kauai, Hawaii, 22 - 25 September 2013.
12. WILKINS, B., 'Statoil Flare Ignition Tests', Kollsnes, 26/8-09, CMR Gexcon Technical Note November, 2009.
13. SAID, R., GARO, A. and BORGHI, R., 'Soot Formation Modeling for Turbulent Flames', Combustion and Flame, Vol. 108, 1997, pp. 71 - 86.
14. MONNOT, G., Principles of Turbulent Fired Heat, Edition Technips, Paris, 1985.
15. DUTERQUE J., ROLAND, B. and HELENE, T., 'Study of Quasi-Global Schemes for Hydrocarbon Combustion', Combustion Science and Technology, 26 (1 - 2), 1 - 15, 1981.
16. KIM, I. K. and MARUTS, K., 'A Numerical Study on Propagation of Premix Flames in Small Tubes', Combustion and Flame, 146, 283 - 301, 2006.
17. LIND, C. D. and WHITSON, J., 'Explosion Hazards Associated with Large Quantities of Hazardous Materials', US Coast Guard Final Report ADA047585, 1977.